Small-angle X-ray scattering from a thermotropic random copolymer during solid-state annealing

D.J. Wilson[+], *S. Seifert, N. Stribeck, A.H. Windle*[++] and *H.G. Zachmann**

Institut für Technische und Makromolekulare Chemie, Universität Hamburg, Bundesstraße 45, D-20146 Hamburg, FRG
[+] Now at Dow Corning Ltd., Cardiff Road, Barry South Glamorgan, CF63 2YL, United Kingdom
[++] Department of Materials Science and Metallurgy, University of Cambridge, Pembroke Street, Cambridge, CB2 3QZ, United Kingdom

This paper reports the effect of solid state annealing on the structure of a liquid crystalline polymer composed of 80% 4-hydroxybenzoic acid (HBA) and 20% 2-hydroxy-6-naphthoic acid (HNA) using small-angle X-ray scattering. Two-dimensional diffraction patterns possessing strong meridional reflections were recorded using synchrotron radiation at temperatures of 215, 251 and 269°C. The long period increased with increasing anneal temperature, but was largely unaffected by increasing the length of time spent at the anneal temperature. The intensity of meridional scattering increased with both increasing anneal temperature and time. In order to obtain an estimate for the average crystallite thickness at the anneal temperature, the small-angle meridional scattering was evaluated by means of the interfacial distribution function approach.

1. Introduction

The aromatic copolyester composed of 4-hydroxybenzoic acid (HBA) and 2-hydroxy-6-naphthoic acid (HNA) has a nematic melt of low viscosity coupled with excellent chemical resistance and thermal stability. It thereby lends itself readily to the manufacture of intricate parts for aggressive environments, such as motor components and fuel rails, and is commercially marketed under the tradename of Vectra [1]. The utilization of this copolymer at elevated temperatures clearly warrants a consideration of the morphological changes which may be expected to occur during heating, but it has not yet been possible to perform electron microscopy under such conditions. Therefore, the technique of high-temperature small-angle X-ray scattering (SAXS) has been employed.

In copoly(HBA/HNA), it is well known from wide-angle X-ray scattering (WAXS) that mid range compositions crystallize as a metastable pseudo-hexagonal structure, which transforms on annealing to an orthorhombic phase. This technique also demonstrates the aperiodicity of the meridional peaks which confirms that the crystallites comprise random sequences in the chain [2, 3]. NMR measurements also confirm that the copolymer is essentially random. Recent work has shown that the appearance of discrete meridional maxima in the small-angle region can be correlated with the development of the orthorhombic structure [4–6]. However, all previous SAXS observations have been made at room temperature after quenching [4–8], and it is important to realize that one of the main aims of this research was to record two-dimensional SAXS patterns at the DESY synchrotron facility without first having to quench from the anneal temperature. In this way, the variation of long period as a function of time during isothermal crystallization could be investigated.

Another objective of the current study has been to quantify the diffraction results in light of recent measurements made by transmission electron microscopy (TEM) [8, 9]. In this respect, copoly(HBA/HNA) has been relatively well investigated and crystallites appear to be present as platelets with their thin axis parallel to the molecular chain axis. Indeed, in low molecular weight copoly(HBA/HNA), the lateral extent of the crystallites may be as much as 20 to 30 times as large as in the vertical direction [10], imparting a semi-lamellar nature. Consequently, interfacial distribution functions (IDFs) were evaluated from the experimentally recorded SAXS curves in order to estimate long periods and crystallite thicknesses at the anneal temperature.

2. Material

The sample is a random copolymer composed of 80% 4-hydroxybenzoate (HBA) and 20% 2-hydroxy-6-naphthoate (HNA) units (referred to as B-N 4:1), with a weight-average molecular weight of 6100 and a melting point of 306 °C. It was kindly supplied by the Hoechst-Celanese Corporation (Summit, NJ, USA).

3. Experimental

Kratky camera measurements were made using nickel-filtered CuK_α radiation, the fiber axis of a sample being perpendicular to the slit collimation system. The small-angle scattering was recorded on Reflex 25 double emulsion film manufactured by CEA, and quantified by scanning on a Joyce-Loebl double-beam microdensitometer.

Synchrotron SAXS was performed on the polymer beamline at Hasylab, DESY in Hamburg. The scattering was detected by means of a Vidicon camera [11, 12] while ramped isothermal annealing treatments were carried out at 215, 251 and 269 °C on a constrained bundle of fibers. The ramping experiment is illustrated schematically in Fig. 1. The same sample was used throughout the 290 min duration of the experiment, and the two-dimensional scattering patterns were collected under vacuum at 1 min intervals. After correction for the electronic background undulations of the detector [13], the scattering patterns were normalized to account for the fall-off in intensity of the primary beam during the measurement period [14]. One-dimensional scattering curves for the evaluation of interfacial distribution functions were obtained by taking vertical sections through the points of highest intensity on the meridian. The resulting intensity profiles were analyzed using a suitably modified version of 'TOPAS', a program distributed by one of the authors for the evaluation of SAXS curves from so-callet 'two-phase' systems [15].

Fax: +49-40-41236008

0323-7648/95/0510-0373$5.00 + .25/0

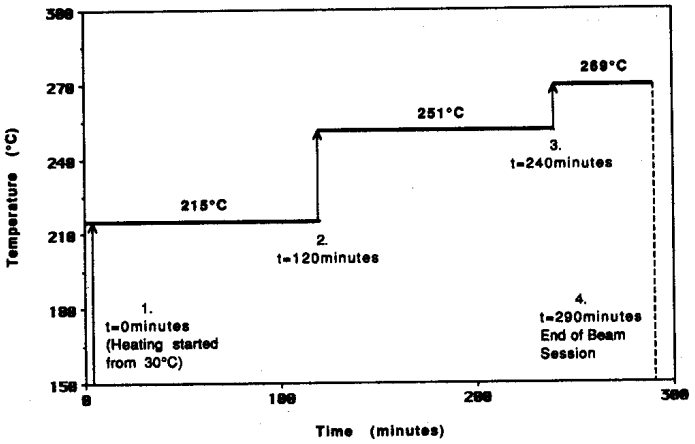

Fig. 1. Schematic illustration of the ramping process employed in the current investigation. The vertical arrows indicate a heating rate of 150 °C/min.

4. Results

4.1 Kratky camera measurements

Diffraction maxima were recorded at room temperature from well-annealed fibers as a function of anneal temperature (Fig. 2). The fibers were placed perpendicular to the slit in the camera. As the anneal temperature increased, the scattered intensity and long period both became larger. The peak maxima yielded long periods of between 32 and 50 nm, the latter value occurring close to the limits of resolution of the polymer beamline at DESY.

4.2. Synchrotron measurements

Figure 3 depicts the two-dimensional scattering pattern from fibers of as-quenched B-N 4:1 at room temperature. Well-developed peaks are apparent on the meridian, in addition to a considerable amount of equatorial scattering.

Figure 4 illustrates the effects of increasing both time and temperature on the scattering patterns of copoly(HBA/HNA) during heating. Distinct meridional maxima are again apparent as a function of increasing anneal times of up to 45 min at 215, 251, and 269 °C. The maxima are evidently rather close to the experimental limit of resolution, but the presence of a discrete reflection was confirmed on an ultra-small-angle scattering beamline at room temperature after annealing for 6 h at 288 °C (Fig. 5).

The background-corrected meridional sections obtained from the diffraction patterns in Fig. 4 at each of the three anneal temperatures, as a function of time, are depicted in Figs. 6 a–c. Long periods obtained from the peak maxima were found to be in the range of 35–50 nm (Fig. 7). It is important to note that the long periods increase with increasing anneal temperature, but that there is no discernible change with increasing anneal time.

The scattering power, Q, in the meridional reflections in Fig. 4 was evaluated, assuming cylindrical symmetry, according to

$$Q = 2\pi \iint I(s_{12}, s_3) \cdot s_{12}\, \mathrm{d}s_{12}\, \mathrm{d}s_3 \qquad (1)$$

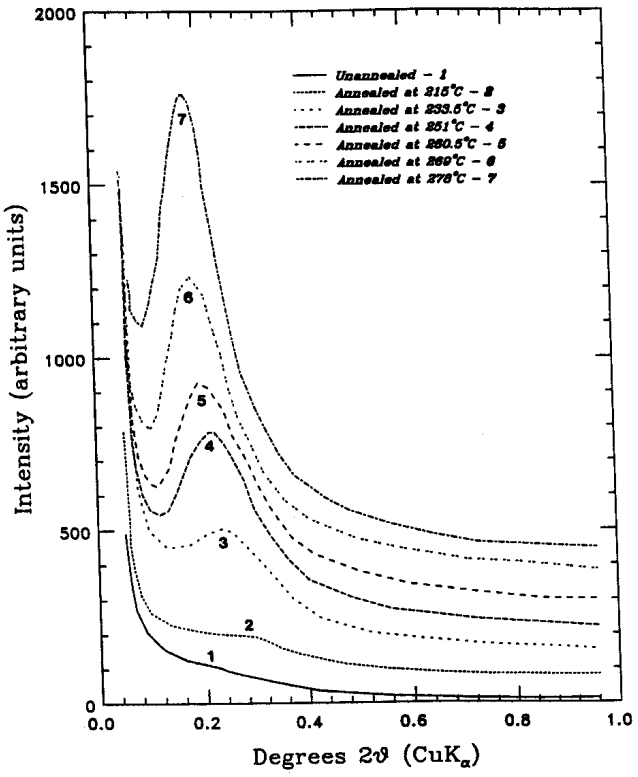

Fig. 2. Meridional SAXS curves obtained at room temperature with a Kratky camera (nickel-filtered CuK_α radiation) for B-N 4:1 after different annealing treatments [5]. Trace 1 is for an unannealed specimen. Traces 2–7 are for samples annealed for 6 h at 215, 233.5, 251, 260.5, 269 and 278 °C respectively. The increase in intensity at low angles represents the overspill from the primary beam. For clarity, subsequent curves have been displaced in the vertical direction. The long periods determined from the peak maxima using Bragg's law are as follows (trace number/small-angle maxima): 1/50 nm; 2/32 nm; 3/39 nm; 4/71 nm; 5/43 nm; 6/47 nm; 7/50 nm.

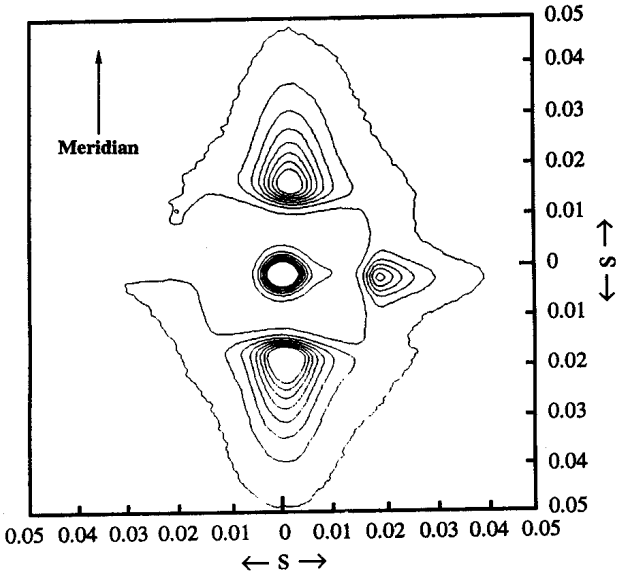

Fig. 3. Two-dimensional scattering pattern for the as-quenched fibers of B-N 4:1 at room temperature, as recorded with a Vidicon detector at DESY. The fiber direction is vertical, and the outer extremes of the contour lines in the meridional direction are approximately equal to $s = 0.05\mathrm{nm}^{-1}$. Lower contour levels were omitted in order to give a clearer representation ($s = 2\sin\theta/\lambda$, $\lambda = 0.15$ nm).

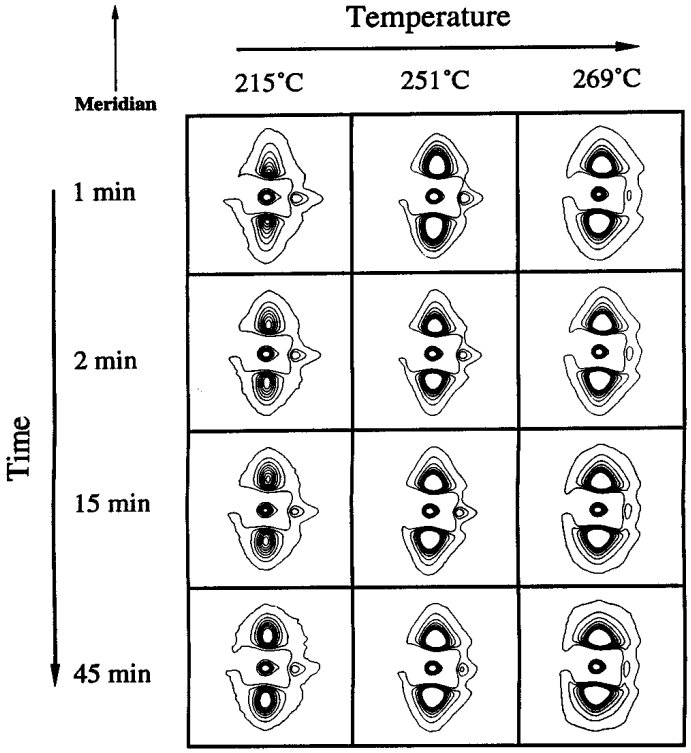

Fig. 4. SAXS patterns for B-N 4:1 after annealing for 1, 2, 15 and 45 min at 215, 251, and 269 °C. Diffraction patterns were recorded at anneal times of up to 100 min at 215 and 251 °C, but no recognizable changes were observed beyond 45 min. The fibre direction is vertical, and the outer extremes of the contour lines in the meridional direction are approximately equal to $s = 0.05$, as in Fig. 3.

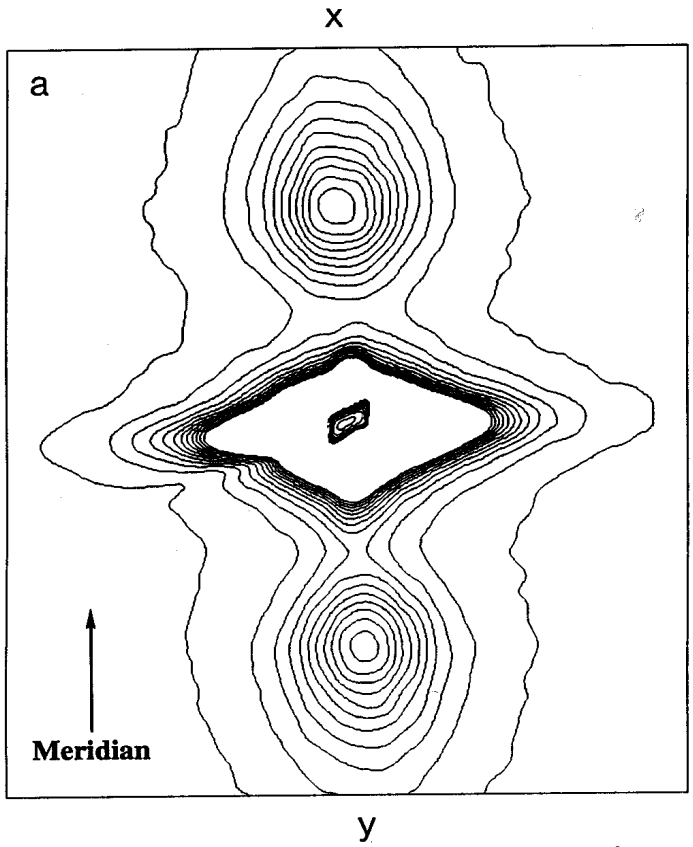

with $I(s_{12}, s_3)$ representing the scattered intensity, and s_{12} and s_3 being the components of the scattering vector s in the equatorial and meridional directions respectively. The resulting integrated meridional SAXS intensity increased gradually with increasing anneal time at 215 °C, while becoming noticeably more intense with time at both 251 and 269 °C (Fig. 8).

In order to estimate a value for the crystallite thickness at the anneal temperature, some of the meridional small-angle scattering patterns were evaluated by means of the interfacial distribution function (IDF) analysis, as introduced by Ruland [16]. The calculation was performed for the scattering curves recorded at 251 °C (Fig. 6b), which not only had an intermediate noise level but were also relatively far from the primary beam-stop. In accordance with the experimental conditions it could be assumed that the synchrotron radiation was point-collimated, and the sample was of uniaxial symmetry. As discussed elsewhere [17–20], the determination of the IDFs then amounted to the calculation of the one-dimensional *interference* function, $G_1(s)$, from which the IDF, $g_1(r)$, could be computed by a Fourier cosine transformation according to

$$g_1(r) = -\int_0^\infty G_1(s) \cdot \cos(2\pi rs)\mathrm{d}s \qquad (2)$$

where r is a distance in real space. The determination of the interference function $G_1(s)$ involves the elimination of two effects in the scattering curves, which originate from imperfections of the "real" two-phase system. The first effect is a background in the scattering curve, which results from statistical fluctuations of the electron density. The second one is a deviation in the slope of Porod's law, which arises from the finite width of the transition zone between the phases.

Due to the poor signal-to-noise ratio in the tail of the meridional sections of the synchrotron 2D patterns, it was not possible to separate the two effects. It was therefore decided to subtract a constant fluctuation background only, in such a way the integral over the resulting interference function was close to zero. The application of Eq. (2) for the evaluation of the meridional SAXS intensity makes the assumption that the orientation and the structure of the lamellar domains are not correlated.

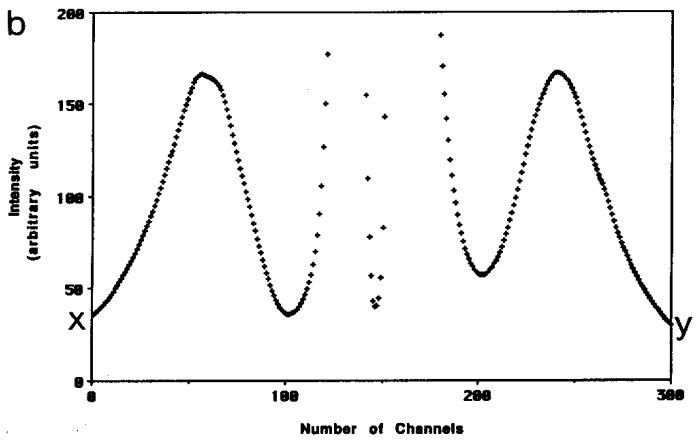

Fig. 5a. Two dimensional SAXS pattern for well-annealed fibers of B-N 4:1 recorded at room temperature on an ultra-small-angle scattering beamline at DESY. The fibre direction is again vertical, parallel to *X–Y*. The sample had previously been annealed for 6 h at 288 °C, and quenched to room temperature. The Bragg long period obtained from the peak maximum is 53 nm ($s = 0.019$.
Fig. 5b. Meridional section through the scattering pattern in Fig. 5a.

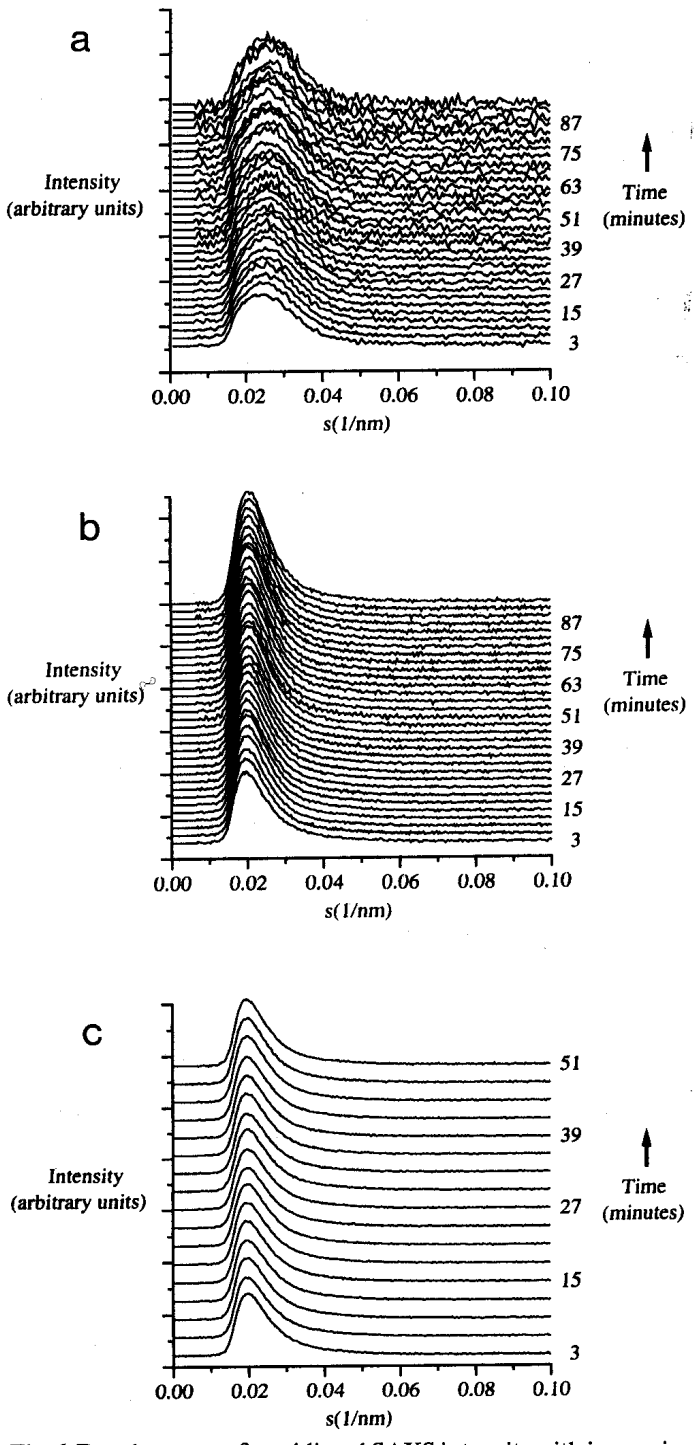

Fig. 6. Development of meridional SAXS intensity with increasing time at (a) 215 °C (b) 251 °C and (c) 269 °C.

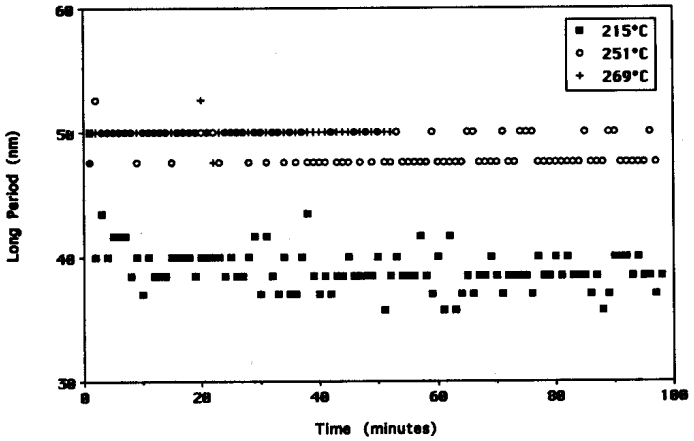

Fig. 7. Long periods versus anneal time at 215, 251, and 269 °C as determined by the application of Bragg's law to the peak maxima of the scattering curves in Fig. 6.

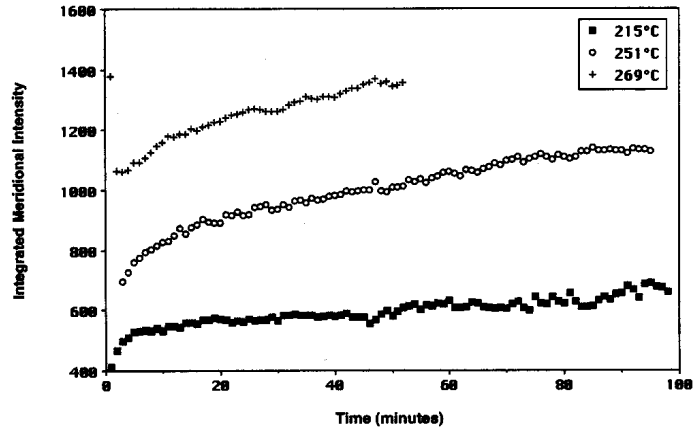

Fig. 8. Integrated meridional intensity versus anneal time at 215, 251, and 269 °C.

Figures 9a and b show the resulting interfacial distribution functions for two scattering curves after 3 and 91 min at 251 °C respectively. In comparison to Fig. 9b, the IDF in Fig. 9a after 3 min appears to show some bimodality, that is, the apparent superposition of two different long period distributions, and this behavior was typical for times of between 2 and 7 min. However, the first data set and all subsequent sets between 8 and 97 min yielded interfacial distribution functions of similar shapes to Fig. 9b.

The experimental $g_1(r)$ curves were then fitted to extract information relating to the crystallite length, l_c, extent of the amorphous phase, l_a, and the long period. A simple homogeneous stacking model was used, in which correlations between three adjacent crystalline lamellae in one-dimensional lamellar stacks were considered [17]. The results of this modeling process are also illustrated in Figs. 9a and 9b (dotted lines), in which the first maximum can be attributed to a combination of the overlapping crystalline and amorphous thickness distributions, and the position of the first minimum is related to the long period. The resulting long periods and crystallite thicknesses for some representative curves between 1 and 97 min at 251 °C are shown in Fig. 10. The long periods determined from the interfacial distribution function approach were generally found to be in the range of 35 to 40 nm, and the crystallite thicknesses had an average value of about 12 nm. The latter result compares favorably with three recent TEM investigations into both low and high molecular weight copoly(HBA/HNA) at room temperature (Table 1).

5. Discussion

Most research on copoly(HBA/HNA) to date has been performed on the B-N 3:1 material, which is pseudo-hexagonal in the as-quenched state and transforms to an orthorhombic structure during annealing. Previous work has shown a correlation between the observation of the phase transformation from the pseudo-hexagonal structure to the

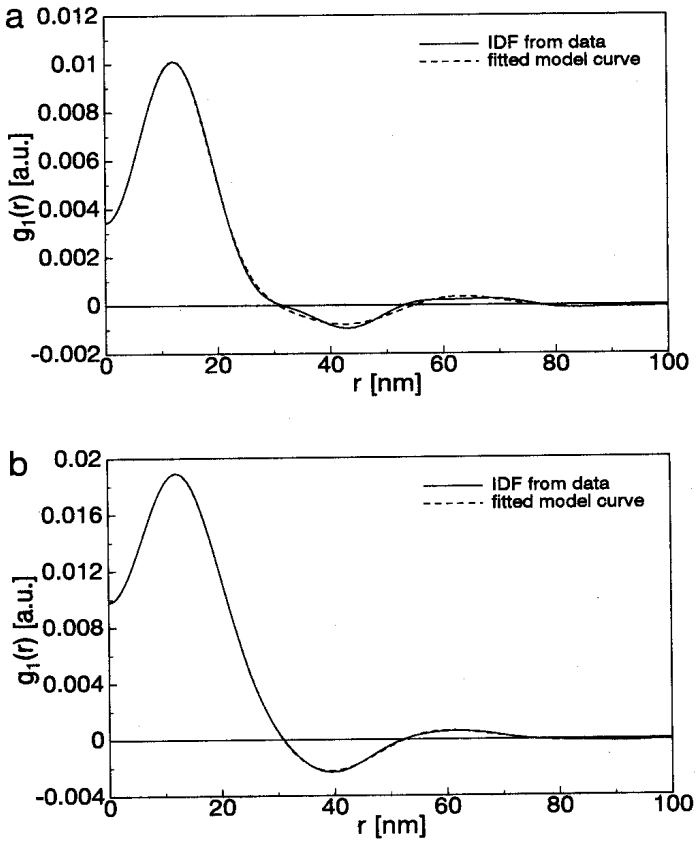

Fig. 9. The interfacial distribution functions (solid lines), $g_1(r)$, after annealing for (a) 3 min and (b) 91 min at 251 °C. The dashed lines correspond to theoretical IDFs, based upon a simple stacking model in which correlations between three adjacent crystalline lamellae were considered.

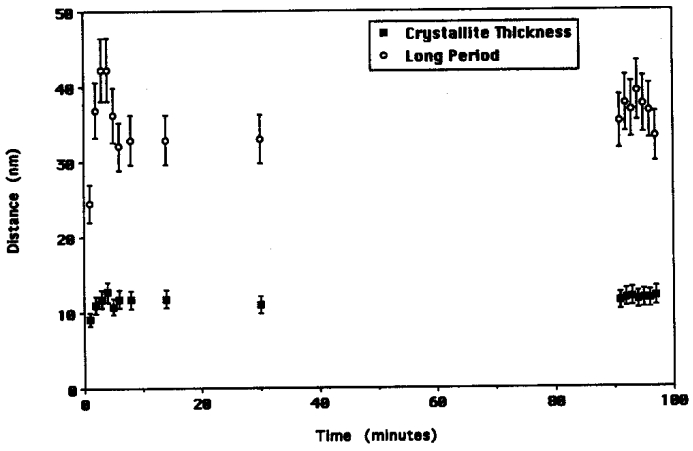

Fig. 10. Crystallite thicknesses and corresponding long periods calculated by the IDF analysis as a function of anneal time at 251 °C.

orthorhombic one and the appearance of discrete meridional maxima in the SAXS patterns of these materials [7]. These data underline the similarity in densities between the pseudo-hexagonal crystals and the nematic phase, at least at room temperature.

In the current investigation, B-N 4:1 was employed, and this sample has been shown to develop the orthorhombic structure on cooling without the need for annealing [7]. The observation of small-angle meridional maxima in these samples (Fig. 3) reflects the difference in density between

Table 1. Previous estimates of crystallite thicknesses determined by a variety of techniques for different compositions and molecular weights of copoly(HBA/HNA). For each method, the results are listed in chronological order.

Method	Composition	D.P.[a]	Crystal thickness [nm]	Ref.
TEM	70:30	High	≤20	21
	70:30	High	≈20	22
	75:25	Low/High	10/20	7
	75:25	Low	10–17	8
	73:27	High	10	23
SAXS + WAXS[b]	75:25	Low	6.3–8.5	8
	80:20 to 67:33	Low-Medium	6–12	6
SEM	75:25	Low	≤75	24
	75:25	Low	18–34	8
Computer modeling	75:25	Low	2.4–8.2	8

[a] Degree of polymerisation: low: ≤50; medium: 50–150; high: ≥150, [b] Derived from (long period × crystalline fraction)

the orthorhombic phase and the surrounding nematic matrix.

Following a sudden increase in temperature to 215 °C, the SAXS pattern is almost unchanged (Fig. 4), and increasing the anneal time has almost no effect upon the long period (Fig. 7). This is a general phenomenon for each of the three anneal temperatures. However, increasing temperature is accompanied by an increase in the overall long period, presumably because this results in a melting out of some intervening crystallites. Experiments in which the long period has been measured as a function of molecular weight [25] show no dependences of the former on the latter.

Annealing leads to an increase in the integrated meridional intensity (Fig. 8). The scattering power for a two-phase system will be proportional to both the product $\varphi(1-\varphi)$ where φ is the volume crystallinity, and to the square of the electron density difference $\Delta\varrho$ between the two phases. Previous work has indicated that the degree of crystallinity is not markedly enhanced by increasing either the anneal time or temperature [7, 9, 26]. Indeed, crystallinity would be expected to decrease slightly as one approaches the melting point, although the highest anneal temperature of 269 °C in this experiment is well below the nominal melting point of the polymer (306 °C), which will in any case have increased during the annealing process. Therefore the increase in SAXS intensity results from the electron density difference term $\Delta\varrho$. An increse in $\Delta\varrho$ will certainly be caused by the different thermal expansion of the crystals and the amorphous regions as observed in other polymers [14]. Furthermore, some changes in $\Delta\varrho$ may arise from the transformation of the pseudo-hexagonal into the orthorhombic phase. By analogy with B-N 3:1, it is known that increasing amounts of the orthorhombic phase are being formed at the expense of the pseudo-hexagonal one.

A final comment on the underlying mechanism controlling the observed changes to crystallite morphology is appropriate. While the observed increase in long period is associated with the melting out of intervening crystallites, the kinetic control on the phase transformation from pseudo-hexagonal to orthorhombic is almost certainly associated with the molecular re-adjustments necessary to accommodate the packing density difference at the ortho-

rhombic crystal-nematic interface, as has been discussed in [26]. It is likely that transesterification processes play an important role in enabling these re-adjustments.

6. Conclusions

1. The 4:1 sample of B-N showed discrete small-angle X-ray diffraction maxima at room temperature and at each of the three anneal temperatures. With increasing temperature during heating, the long period was observed to increase, which mirrors to behavior of samples which were quenched to room temperature after annealing [7]. However, the long period is not markedly changed by annealing for times of up to 100 min, suggesting that long-term heat treatment does not lead to the formation of new crystallites between pre-existing ones, or that if this process does occur, then new crystallites form in such a way as to maintain an optimum long period for a particular anneal temperature. This behavior is similar to that of homopolymers with flexible chains such as polyethylene, poly(ethylene terephthalate), poly(ethylene naphthalene-2,6-dicarboxylate) and poly(aryl ether ether ketone) [27–30], in which an increase or decrease in the long period is often observed at short times, depending upon thermal history, and after which no significant change is registered.

2. The integrated *meridional* SAXS intensity was found to increase significantly during annealing at higher anneal temperatures. This is thought to be related to the density contrast resulting from the transformation of the less dense pseudo-hexagonal phase into the more dense orthorhombic crystalline modification.

3. Crystallite thicknesses determined by the interfacial distribution function approach were found, at 251 °C, to be unchanged during annealing, with an average value of about 12 nm.

Acknowledgements

The authors are indebted to Dr. M. Bark of the ultra-small-angle scattering beamline at Hasylab, and to Dr. C. Zschunke for a number of informative discussions during the preparation of this manuscript. One of us (DJW) also wishes to thank the Royal Society for a Postdoctoral Research Fellowship.

References

[1] "Vectra, Liquid Crystal Polymer: Automotive Industry Applications (VC-8)", Engineering Plastics Division, Hoechst-Celanese Corporation **1988.**

[2] J. Blackwell, G.A. Gutierrez, R.A. Chivers, *Macromolecules* **1984,** *17,* 1219.

[3] G.R. Mitchell, A.H. Windle, *Colloid Polym. Sci.* **1985,** *263,* 230.

[4] D.J. Wilson, C.G. Vonk, A.H. Windle, *IUPAC International Symposium Preprints,* Royal Australian Chemical Institute **1991.**

[5] D.J. Wilson, *PhD Thesis,* University of Cambridge **1992.**

[6] D.J. Wilson, C.G. Vonk, A.H. Windle, *Polymer* **1993,** *34,* 227.

[7] C. Viney, A.H. Windle, *Mol. Cryst., Liq. Cryst.* **1985,** *129,* 75.

[8] S. Hanna, T.J. Lemmon, R.J. Spontak, A.H. Windle, *Polymer* **1992,** *33,* 3.

[9] R.J. Spontak, A.H. Windle, *Polymer* **1990,** *31,* 1395.

[10] R.J. Spontak, A.H. Windle, *J. Mater. Sci.* **1990,** *25,* 2727.

[11] W. Prieske, C. Riekel, M.J. Koch, H.G. Zachmann, *Nucl. Instrum. Methods* **1983,** *208,* 435.

[12] G. Elsner, C. Riekel, H.G. Zachmann, *Adv. Polym. Sci.* **1985,** *67,* 1.

[13] P. Bösecke, D. Ercan, C. Riekel, *J. de Phys.* **1986,** *Colloque C5,* 175.

[14] R. Gehrke, C. Riekel, H.G. Zachmann, *Polymer* **1989,** *30,* 1582.

[15] N. Stribeck, *Colloid Polym. Sci.* **1993,** *271,* 1007.

[16] W. Ruland, *Colloid Polym. Sci.* **1977,** *255,* 417.

[17] N. Stribeck, W. Ruland, *J. Appl. Crystallogr.* **1978,** *11,* 535.

[18] W. Wenig, T. Schöller, *Angew. Makromol. Chem.* **1985,** *130,* 155.

[19] H.W. Fiedel, W. Wenig, *Colloid Polym. Sci.* **1989,** *267,* 389.

[20] C. Santa Cruz, N. Stribeck, H.G. Zachmann, F.J. Baltá Calleja, *Macromolecules* **1991,** *24,* 5980.

[21] A.H. Windle, C. Viney, R. Golombok, A.M. Donald, G.R. Mitchell, *Faraday Discuss. Chem. Soc.* **1985,** *79,* 55.

[22] A.M. Donald, A.H. Windle, *J. Mater. Sci. Lett.* **1985,** *4,* 58.

[23] S.D. Hudson, A.J. Lovinger, *Polymer* **1993,** *34,* 1123.

[24] T.J. Lemmon, S. Hanna, A.H. Windle, *Polym. Commun.* **1989,** *30,* 1.

[25] A. Anwer, A.H. Windle, *Polymer* **1993,** *34,* 3347.

[26] S. Hanna, T.J. Lemmon, in *Polymer Science: Contemporary Themes,* Vol. 2, (Ed: S. Sivaram), Tata McGraw-Hill, New Delhi **1991,** p. 504.

[27] G. Elsner, M.J.H. Koch, J. Bordas, H.G. Zachmann, *Makromol. Chem.* **1981,** *182,* 1263.

[28] M. Bark, H.G. Zachmann, R. Alamo, L. Mandelkern, *Makromol. Chem.* **1992,** *193,* 2363.

[29] H.G. Zachmann, C. Wutz, in *Crystallisation of Polymers* (Ed.: M. Dosière), Kluwer Academic, Dordrecht, The Netherlands **1993.**

[30] B.S. Hsiao, K.H. Gardner, D.Q. Wu, B. Chu, *Polymer* **1993,** *34,* 3986.

Received October 6, 1994

Final version June 20, 1995